Integrated Approach for Steam Turbine Thermostructural Analysis and Lifetime Prediction at Transient Operations

Leonid Moroz
SoftInWay, Inc.,
1500 District Avenue,
Burlington, MA 01803
e-mail: L.Moroz@softinway.com

Glenn Doerksen
Sulzer Turbo Services Houston Inc.,
11518 Old La Porte Road,
La Porte, TX 77571
e-mail: glenn.doerksen@sulzer.com

Fernando Romero
Sulzer Turbo Services Houston Inc.,
11518 Old La Porte Road,
La Porte, TX 77571
e-mail: fernando.romero@sulzer.com

Roman Kochurov[1]
SoftInWay, Inc.,
1500 District Avenue,
Burlington, MA 01803
e-mail: R.Kochurov@softinway.com

Boris Frolov
SoftInWay, Inc.,
1500 District Avenue,
Burlington, MA 01803
e-mail: boris.frolov@softinway.com

In order to achieve the highest power plant efficiency, original equipment manufacturers continuously increase turbine working parameters (steam temperatures and pressures), improve components design, and modify start-up cycles to reduce time while providing more frequent start-up events. All these actions result in much higher levels of thermostresses, a lifetime consumption of primary components and an increased demand for accurate thermostructural and low cycle fatigue (LCF) simulations. In this study, some aspects of methodological improvement are analyzed and proposed in the frame of an integrated approach for steam turbine components thermostructural analysis, reliability, and lifetime prediction. The full scope of the engineering tasks includes aero/thermodynamic flow path and secondary flows analysis to determine thermal boundary conditions (BCs), detailed thermal/structural two-dimensional and three-dimensional (3D) finite element (FE) models preparation, components thermal and stress–strain simulation, rotor–casing differential expansion and clearances analysis, and finally, turbine unit lifetime estimation. Special attention is paid to some of the key factors influencing the accuracy of thermal stresses prediction, specifically, the effect of "steam condensation" on thermal BC, the level of detailing for thermal zones definition, thermal contacts, and mesh quality in mechanical models. These aspects have been studied and validated against test data, obtained via a 30 MW steam turbine for combined cycle application based on actual start-up data measured from the power plant. The casing temperatures and rotor–stator differential expansion, measured during the commissioning phase of the turbine, were used for methodology validation. Finally, the evaluation of the steam turbine HPIP rotor lifetime by means of a LCF approach is performed. [DOI: 10.1115/1.4037755]

1 Introduction

Steam turbine accelerated start and operation flexibility together with long-term service life are the most desired and conflicting requirements for the unit operation. Starting the turbine quickly can save fuel cost but results in premature component failure due to low cycle fatigue (LCF).

The main factor that limits turbine start-up time is thermal stresses. Thermal stresses occur in the turbine rotor and casing components (mostly high pressure (HP) and intermediate pressure (IP) cylinders) resulting in LCF and lifetime reduction. Cyclic life evaluation is based on the thermostresses analysis and requires a high level of finite element (FE) model detailing in order to predict stress concentration in the fillets, grooves, etc. The details on thermal stresses initiation due to transient operation can be found in Ref. [1]. Another limiting factor is the differential rotor–casing expansion, which may lead to critical clearances reduction and damage.

For steam turbine components, the thermal state is strongly influenced by the condensation process, which takes place primarily during the initial phase of cold start-up (CS) and continues until the rotor surface temperature becomes higher than the steam saturation temperature. Effect of "condensation" on thermal stresses depends on rotor and casing initial temperatures and steam conditions. When starting up from ambient metal temperature (pure CS), the condensation provides increased speed of components temperature growth and consequently highest stresses. This effect becomes weaker with the metal initial temperature getting closer to steam saturation temperature.

Convection condition accuracy and, especially, the effect of steam condensation during CS, are the key factors to realistically predict turbine unit thermal state during transients.

The fundamentals of heat and mass transfer processes and basic principles of heat transfer coefficient (HTC) simulation are considered in the monographs [2,3].

The pioneer work about film condensation for pure vapor is published by Nusselt [4]. He considered smooth and uniform liquid film on the wall surface and expressed condensation heat transfer coefficients as a ratio of thermal conductivity and thickness of laminar film condensate. A large number of correlations for predicting heat transfer coefficients during film condensation inside pipes have been proposed over the last 80 yr described in Refs. [5–7] and many other publications, where Nusselt correlations were improved and experimentally validated. The simple dimensionless correlation which has been verified by comparison with a wide variety of experimental data is developed in Ref. [5]. Experimental analysis of steam condensation in the vertical tube and HTC comparison against theoretically calculated results is performed in Ref. [6]. Some recommendations based on a summary of calculated and experimental data are presented in Ref. [7]. Based on the results presented in these articles, the condensation HTCs are significantly higher than that of dry conditions and could reach up to 12,000 $W/(m^2 K)$.

Despite the fact that for steam turbine components condensation effect imposes most of the uncertainty that exists for thermostructural analysis, there is very limited published information on condensation HTC simulation methodology and experimental results. Some theoretical approaches to account for the effect of condensation on HTC in different parts of steam turbine

[1]Corresponding author.

Contributed by the Turbomachinery Committee of ASME for publication in the Journal of Engineering for Gas Turbines and Power. Manuscript received July 17, 2017; final manuscript received July 18, 2017; published online October 3, 2017. Editor: David Wisler.

components and validation against test data can be found in monographs [8] and [9].

Basic principles and methodology for steam turbine service life prediction based on its thermal state were developed in Ref. [10]. In Ref. [11], a list of studies performed until the year 2015 for steam turbine components thermomechanical analyses methodology with finite element analysis (FEA) approach and a brief review is given. Valuable results also with regard to experimental validation published in Ref. [12], where conjugate heat transfer numerical models are compared against experimental data of a large intermediate pressure steam turbine module. Cold start-up analysis for IP steam turbine rotor is performed in Ref. [13], and probabilistic sensitivity study was done in order to identify the influence of boundary conditions (BCs) uncertainty on the calculated lifetime consumption for the rotor.

Based on the published works, it can be concluded that thermostructural methodology for steam turbine components is well developed. But not enough information is given with regard to some specific details on condensation thermal boundary conditions, like, for example, start/finish time of condensation for each thermal zone, the impact of condensation on thermal stresses and cyclic life. Most of the known recommendations on condensation effect focused on HTC adjustment with a proper correction function, based on experimental validation.

In this paper, the authors made attempt to improve the accuracy of steam turbine thermostructural analysis by condensation effect consideration with a new proposed differential algorithm to determine condensation start/finish time for each specific thermal zone. Another aspect of accuracy improvement is an integrated approach when all steps of thermostructural analysis are completed within turbomachinery design platform. This integrated approach consists of the following major steps:

(1) direct calculation of steam parameters in turbine flow path at each time-step during start-up cycle with 1D aerothermodynamic solver along with rotor gland seal scheme leakages balance. This approach allows capturing with high accuracy steam parameters variation in the turbine flow path and seal zones and determining "dry" and "saturation" steam properties, the effect of "Windage" at low flow conditions. Flow parameters and steam properties are used for thermal BC (HTC and temperatures) calculation at preliminary assigned thermal zones.
(2) transient thermal analysis for casing and rotor components based on thermal BC, which are automatically transferred from aerosolver module to FEA model. An improved interactive algorithm is applied at this step to the thermal analysis to distinguish "noncondensation" and condensation conditions and to account for the condensation effect.
(3) thermostructural analysis for start-up cycle.
(4) differential expansions analysis.
(5) stresses and lifetime evaluation.

The proposed algorithm was applied to a 30 MW steam turbine during turbine redesign to predict components stresses and clearances behavior at transient operations and also used to develop optimized start-up cycle. The measured data on casing temperatures and rotor–stator differential expansion were used to validate the calculation methodology.

This article represents a continuation of work on this turbine analysis, with the first part published in Ref. [11], where the thermostructural analysis methodology was applied to a rotor only. In this part, the whole steam turbine unit is considered which is mandatory to predict rotor–casing differential expansions.

2 Background

The project involved the conversion of three steam turbines from simple steam oil-fired to natural gas-fired combined cycle. The project was led by Sulzer Turbo Services Houston, Inc. (La Porte, TX), which was responsible for steam turbine redesign and manufacture in cooperation with SoftInWay, Inc., (Burlington, MA) engineering team. The turbines upgrades have been performed for three similar 30 MW steam turbine units (see Figs. 1 and 2) to adjust for operation at combined cycle parameters and to improve efficiency and performance.

The following upgrade options have been applied to the steam turbine in comparison with original design:

(1) new flow path for HPIP and low pressure (LP) turbines with high efficient rotor and stator blades;
(2) upgraded end-packing and blading seals—resulted in new reduced clearances;
(3) modified design and off-design conditions, optimized for combined operation;
(4) modified start-up curves to reduce startup time; and
(5) HPIP rotors from a new material with better mechanical properties.

All these design changes required the full scope of thermomechanical analyses which are presented here by the example of the steam turbine cold start-up.

Some of the steam turbine operating parameters for the design point are presented below:

(1) rotor nominal speed: 3600 rpm;
(2) steam inlet temperature before valves: 505 °C;
(3) steam inlet pressure before valves: 79 bar;
(4) condenser pressure: 0.098 bar.

Actual start-up curves for cold, warm, and hot start-up and shut down operations were taken from the power plant and used for methodology validation. As an example, a cold start-up diagram for the turbine is presented in Fig. 3.

3 Integrated Approach and Methodological Aspects for Turbine Unit Thermostructural Analysis

All steps, typically performed for rotor and casing components thermostructural analysis and lifetime evaluation, are shown in Fig. 4.

Turbine flow path geometry preparation, aerothermodynamic analyses along with rotor gland seal leakages balance and thermal boundary conditions generation are done within integrated turbomachinery design platform [14]. Corresponding thermostructural analyses steps are performed in commercial FEA software with automatic data exchange between these two parts. The advantages of such an integrated iterative procedure are the acceleration of the process and higher accuracy by means of local thermal zones/time-steps refinement.

3.1 Flow Parameters Simulation. As a first step, flow parameters and steam properties in the flow path and rotor gland seals/chambers are determined by *direct* 1D *aerothermodynamic* solver for each time-step.

One of the commonly accepted approaches is based on design point HTC, scaled to each time-step parameters proportionally to

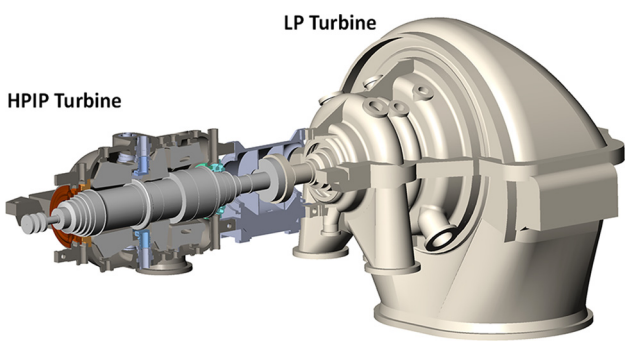

Fig. 1 Thirty megawatt steam turbine model

Fig. 2 Thirty megawatt steam turbine unit—photo from power plant

pressure and temperature ratios [15]. By this way, no condensation and Windage effects could be determined for transient operation.

Figure 5 demonstrates the turbine flow path integrated with gland seal system, which is analyzed for each time-step in 1D aerothermodynamic solver and accounts for main stream and leakages balance, "dry" and "saturated" steam properties, temperature rise because of "Windage". The effect of "Windage" occurs at some regimes, characterized by low flow and high speed with turbine stages operated at "compressor" mode. In this case, solver accounts for some additional energy added to the steam providing temperature rise and changing HTC.

Steam properties and HTC at each thermal zone are calculated and prepared for automatic transfer to FEA thermostructural modules.

To simulate heat convection conditions, HPIP, LP rotors, and all casing components' surfaces were split into *thermal zones* with convection conditions identical or very close within each zone—see Figs. 6 and 7.

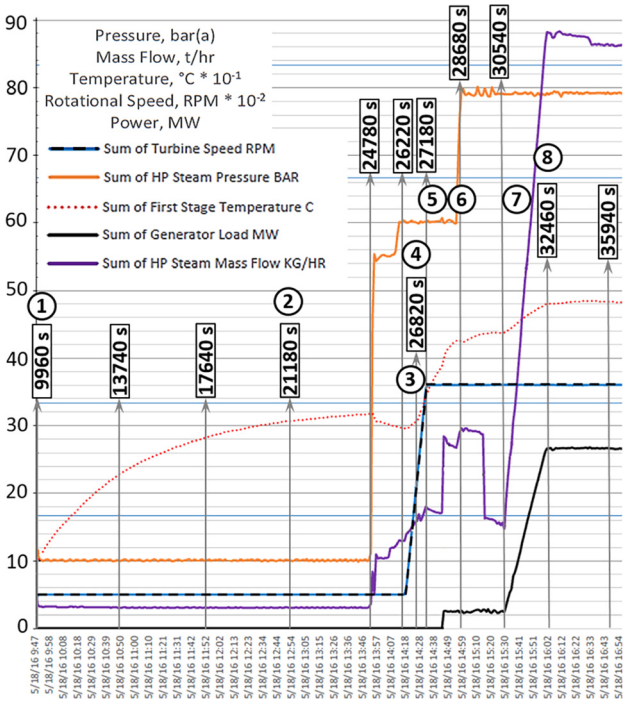

Fig. 3 Cold start-up diagram with calculation time-steps

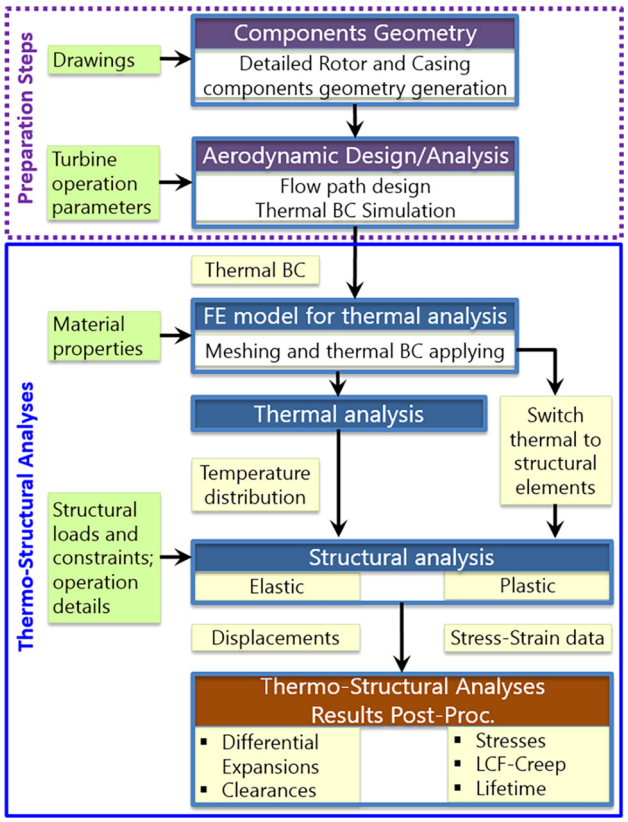

Fig. 4 Thermostructural analysis flow chart

Thermal BC at main flow path, shaft packing zones, and rotor ends/bearings zones are calculated and automatically transferred to the rotor thermostructural FE model at each time-step. On this figure, each zone with unique initial thermal conditions is marked by the corresponding number.

In the 1D aerothermodynamic solver, thermal BC's are calculated for discrete zones with similar local flow properties within each turbine stage at the tip and hub walls. As an example, thermal BC zone assignments for a typical reaction steam turbine stage are presented in Fig. 8.

3.2 Heat Transfer Simulation. *Heat transfer calculation* for convection surfaces of rotors and casing components is based on the classical approach [2,3,8,9] and given by the Dittus–Boelter equation for turbulent pipe flow as follows:

$$\mathrm{HTC} = \mathrm{Nu} \cdot \frac{k}{D_h} \tag{1}$$

where k is the thermal conductivity, and D_h is the hydraulic diameter. Nusselt number can be determined as

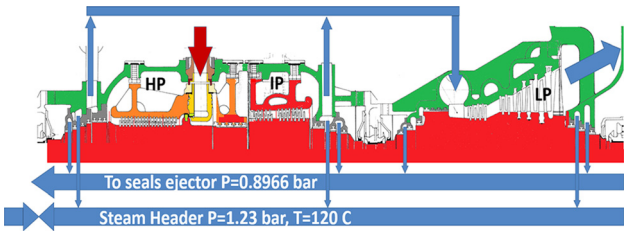

Fig. 5 Turbine flow path integrated with rotor gland seal system for 1D aerothermodynamic analysis

$$\mathrm{Nu} = K \cdot \mathrm{Re}^{0.8} \cdot \mathrm{Pr}^{0.333} \tag{2}$$

where K is the coefficient, determined by convective heat exchange conditions. Reynolds number is calculated using following formulas:

$$\mathrm{Re} = V_{\mathrm{tot}} \cdot \frac{D_h}{(\mu \cdot V)} \tag{3}$$

$$V_{\mathrm{tot}} = \sqrt{V_{ax}^2 + V_{\mathrm{rel}}^2};\ V_{\mathrm{rel}}^2 = XK \cdot \omega \cdot r;\ \ V_{ax}^2 = \frac{G}{\pi\rho\left(r_{\mathrm{ext}}^2 - r_{\mathrm{in}}^2\right)} \tag{4}$$

where V_{tot} is the velocity of steam relative to rotor surface, XK is the coefficient, which considers influence of velocity profile in the gap between rotating and nonrotating surfaces, ω is the rotational speed, r is the cylindrical surface radius, G is the steam mass flow rate, ρ is the steam density, r_{ext} is the external surface radius, r_{in} is the internal surface radius, μ is the steam viscosity, and V is the specific volume.

Convection conditions, which are calculated for stage zones presented in Fig. 8, were averaged for tip and hub walls according to discretization in Figs. 6 and 7. This high level of zone discretization provides sufficiently accurate results.

3.3 Algorithm for Thermal BC Setup. To account for the effect of condensation, two types of thermal conditions are considered—noncondensation and condensation. Noncondensation conditions are determined by "dry" steam properties and the above-mentioned Eqs. (1)–(4) for HTCs. For condensation BCs, a different approach for HTCs simulation is used [7,8], and steam saturation temperature is considered. The interactive algorithm in Fig. 9 was applied as a part of the steam turbine components structural analysis to predict condensation phenomenon.

The approach in Fig. 9 is based on rotor metal temperature monitoring during the transient process and allows us to distinguish the condensation phenomenon with a high level of accuracy with setting condensation versus noncondensation thermal boundary conditions for each local zone at each time-step.

The initial temperature conditions for turbine components depends on previous turbine operation history—it could be cold, warm, or hot [16] and is used to start the calculation process. The initial thermal state could be a strong contributor to the thermostress development and requires an accurate definition. In most cases, the initial thermal distribution in turbine components is not uniform, especially if warm or hot start-ups are considered. To recreate the initial temperature distribution, the thermostructural analysis of turbine cooling from the previous steady-state conditions is required. Another way is based on measured data by installed thermocouples and probes from power plant—initial metal temperature is determined based on casing temperatures and expansion and rotor–stator differential expansions.

Another critical aspect of the proposed process is to compare metal temperature at each local thermal zone against steam

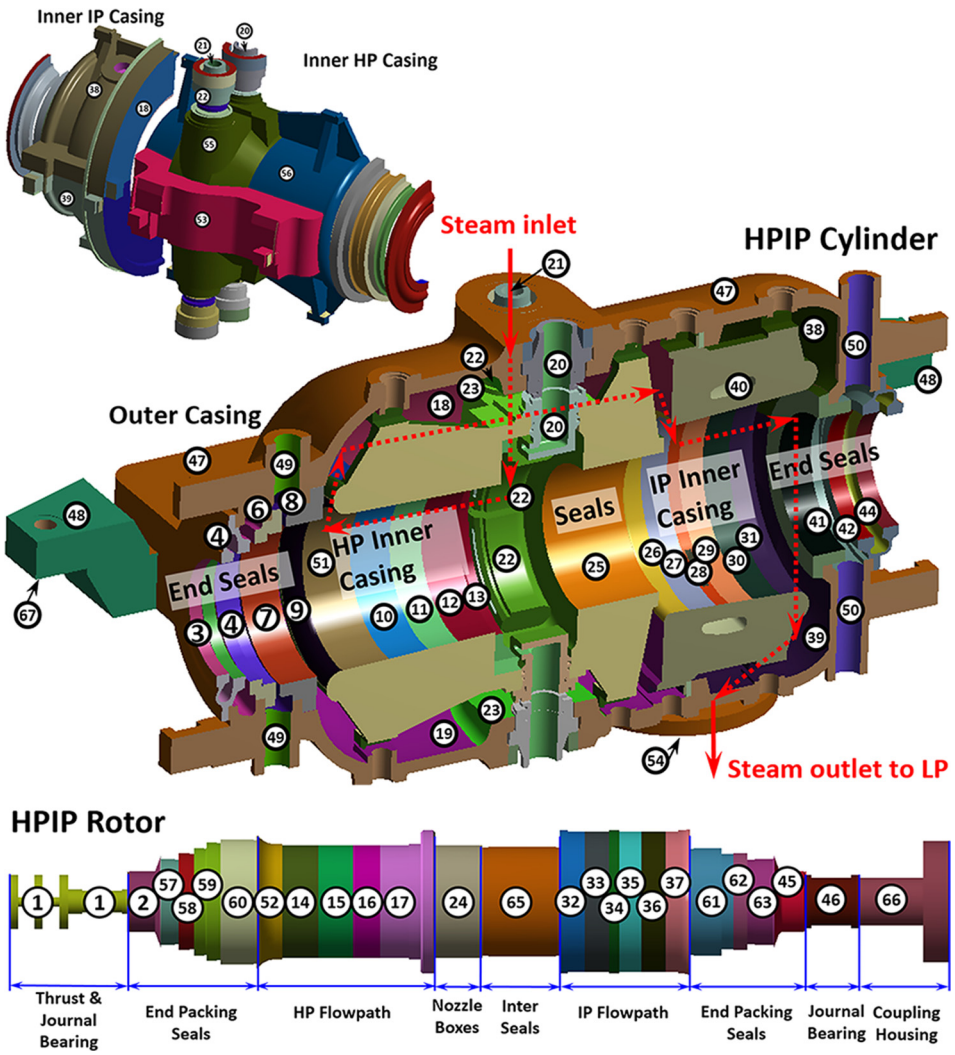

Fig. 6 HPIP turbine heat convection zones discretization and flow direction

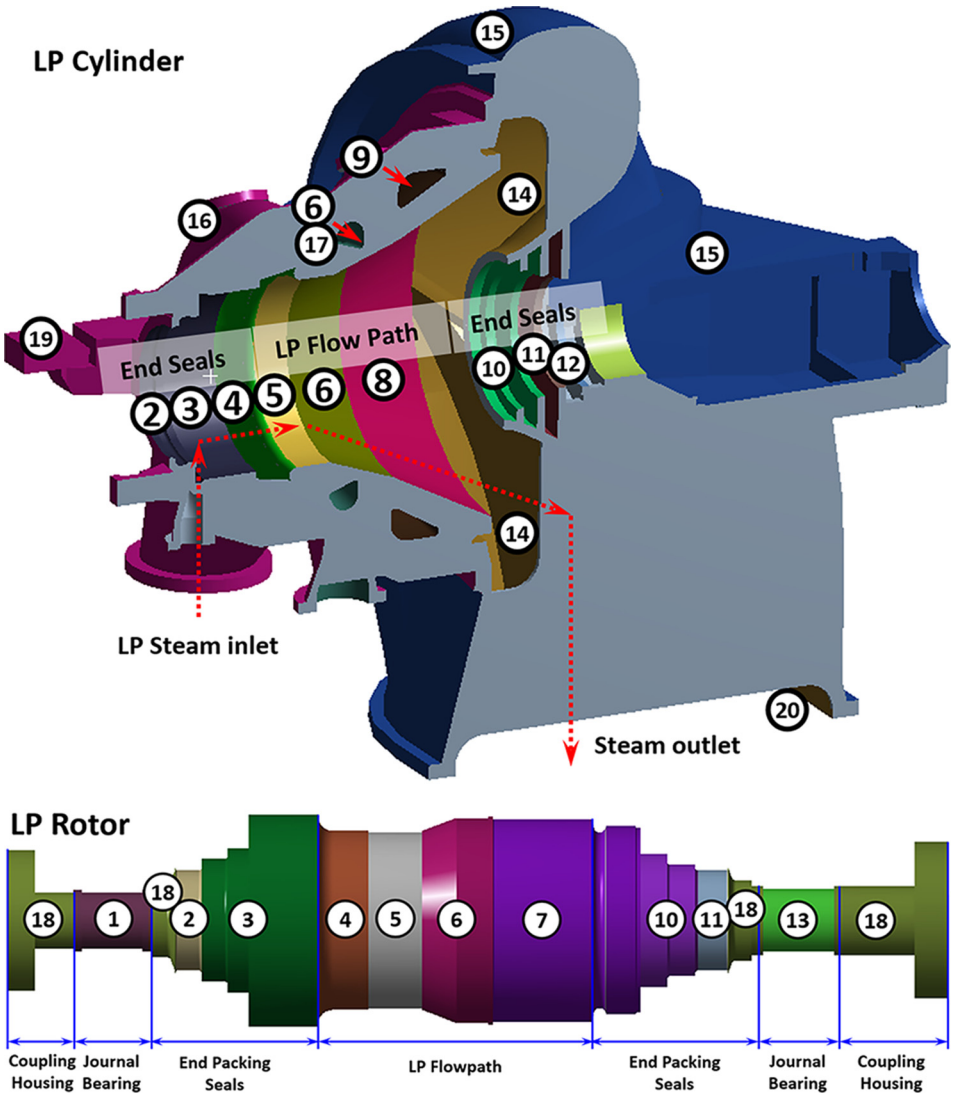

Fig. 7 LP turbine heat convection zones discretization and flow direction

saturation temperature. If local saturation temperature for any zone is higher than that of local rotor metal temperature, we assume that a condensation process occurs. In this case, condensation HTC and steam saturation temperature are applied to this zone.

3.4 FE Mechanical Model. Three-dimensional (3D) FE models based on tetrahedral ten-node and hexahedral 20-node thermal and structural elements have been developed for the casing components. Due to structure symmetry, only half parts of HPIP and LP cylinders were modeled and symmetry conditions were applied—see Fig. 10.

For the turbine HPIP and LP rotors axisymmetric two-dimensional models based on eight-node quadrilateral plane elements (with axisymmetric option) have been developed for transient thermal and structural FE analyses—see Fig. 11, where mesh details for HPIP rotor are presented.

Mesh refinements were done in the regions of potential stress concentration—rotor disk and casing filets, dovetail grooves, etc. HPIP rotor regions with anticipated maximal thermal gradients and stresses (critical zones with regards to LCF crack initiation) are indicated by numbers 1–7 in Fig. 11 and will be used for the further detailed study presented in this article.

In the mechanical models, special focus was paid to adequate thermal contacts modeling between blades and rotor and between

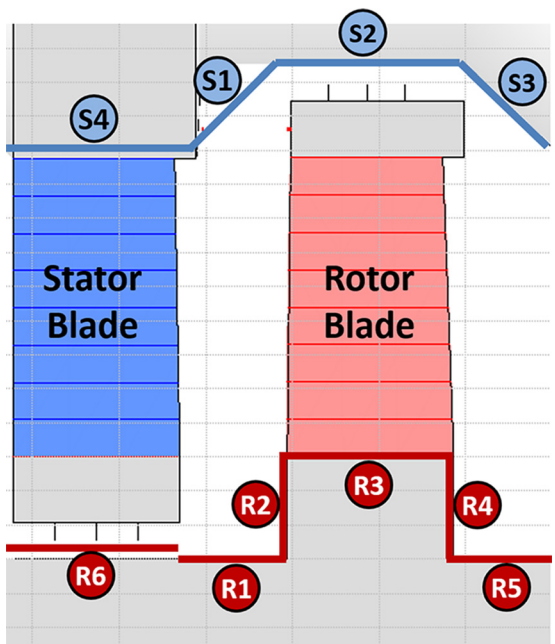

Fig. 8 Flow path stage heat convection zones schematization

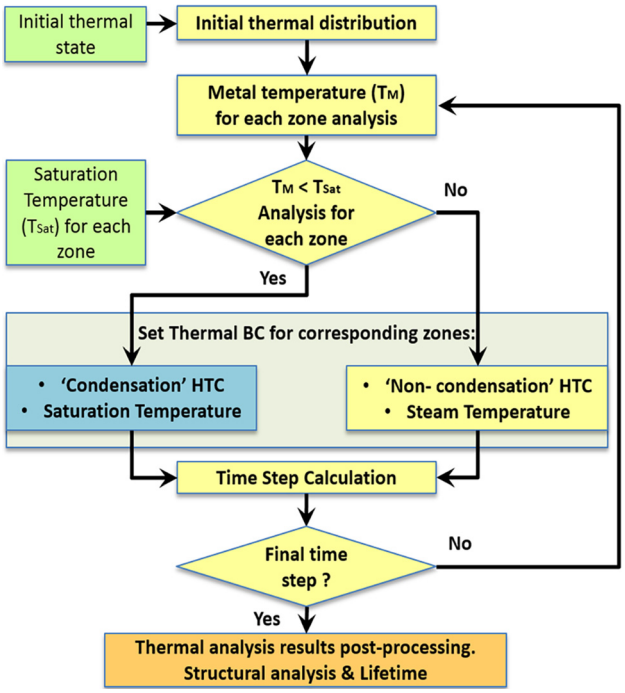

Fig. 9 Algorithm for thermal condensation/noncondensation BC setup for transient analysis

inner and outer casings—see Fig. 12. Convection conditions were applied to blades' platforms as shown in Fig. 12, and thermal resistance at blade root to rotor contacts significantly reduce heat flux to the rotor. Two variants of rotor thermal analysis were completed—with and without thermal contacts, which demonstrated the noticeable difference in rotor–stator differential expansion behavior. Validated against measured expansion data, FE models with thermal contacts demonstrated much better agreement and were used for the final analysis.

An automatic process for convection conditions export from aero/thermodynamic analysis module and applying onto FE mesh was developed and used to accelerate analysis process and eliminate possible errors at this step.

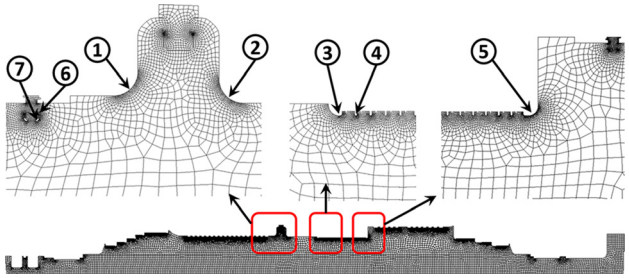

Fig. 11 FE model for HPIP turbine rotor

3.5 Thermal Analysis. Thermal analysis for the steam turbine components is performed based on the algorithm in Fig. 9 and convection conditions, calculated following the procedure described above. For transient thermal analysis, cold, warm, and hot start-up and shut down operations were considered. The only cold start-up results presented in this article, which is based on the actual start-up diagram presented in Fig. 3.

For the current start-up cycle, the initial casing and rotor metal temperatures were re-created by stead-state and shut down simulation with following natural cooling analysis to satisfy both initially measured data:

For casings—measurements of initial casing temperatures and expansions.
For rotor—initial rotor–casing differential expansion measurements.

3.6 Structural Analysis and Lifetime Assessment. Structural analysis is performed for two main purposes:

(1) to evaluate rotor to casing differential expansion; and
(2) to calculate thermostress–strain state and lifetime for critical turbine components.

Structural boundary conditions and rotor centrifugal loads were considered in the analysis. The transient temperature distribution, calculated earlier, is applied to the structural FEA model as the thermal load at appropriate time-steps.

At the first step, the structural analysis is done in a linear (elastic) formulation based on the calculated turbine thermal state

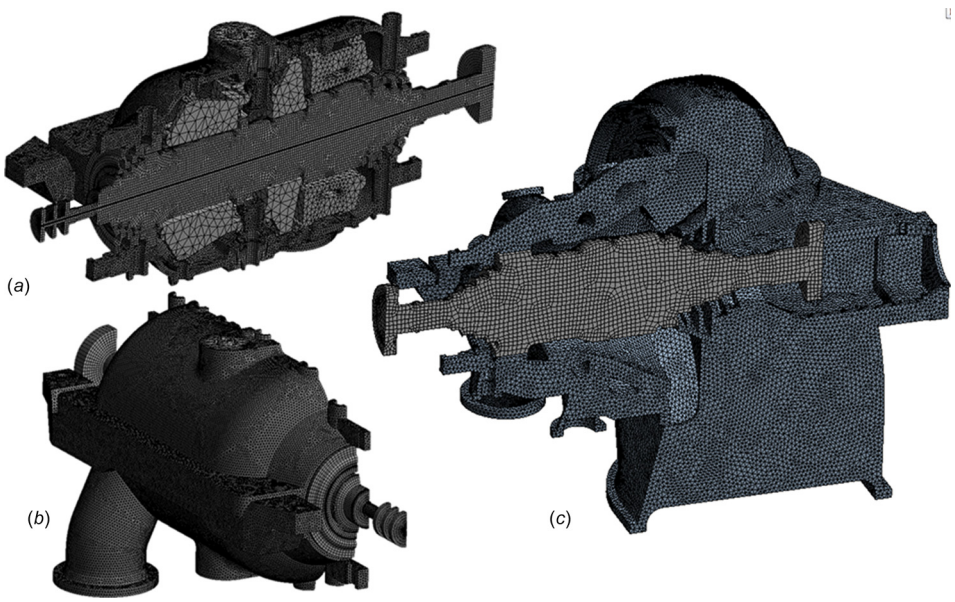

Fig. 10 Three-dimensional FE mechanical models: (*a*) and (*b*) HPIP; (*c*) LP cylinders

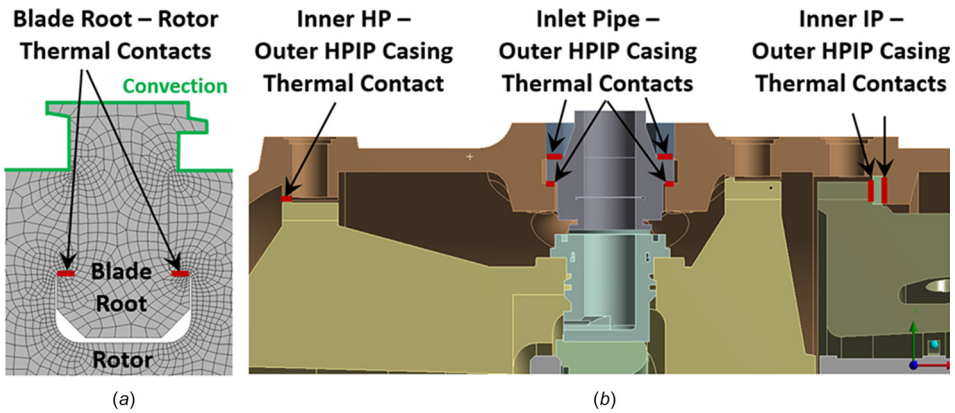

Fig. 12 Thermal contacts modeling: (*a*) blade root-to-rotor and (*b*) HPIP casing components thermal contacts

during a transient start-up process. The elastic analysis gives sufficient accuracy for differential expansion problem and helps to determine the level of stresses and critical time periods. This information from the elastic pass is used to tune-up the algorithm for further nonlinear plastic analysis [11] which results are used for thermostresses and LCF lifetime analysis.

The effect of plasticity was modeled for HPIP rotor following such input data and assumptions:

(1) Actual rotor material stress–strain curves at room and elevated temperature conditions are used.
(2) The rotor material is cyclically hardened. A multilinear kinematic hardening plasticity model is applied.
(3) The nonlinear analysis model includes the Bauschinger effect and geometrical nonlinearity.
(4) Two full cycles of rotor transient plastic stress analyses were performed in series: start-up—running—shut down—to reach stabilized stress–strain hysteresis loops for each region of interest.

One of the rotor life limiting factors is thermomechanical fatigue due to varying stresses during transient operation. Another contributor to limiting rotor lifetime in the high-temperature applications is a creep. The current article is focused on the effect of LCF estimation only and creep effect is not considered in the present study.

Low cycle fatigue analysis is performed based on calculated thermomechanical stress–strain state prediction in a nonlinear plastic statement and experimental strain-life (ε–N) curves for components' material. The theoretical aspects and details for LCF analysis can be found in Ref. [1], and the procedure was described in Ref. [11].

4 Thermal and Differential Expansions Simulation Results and Validation Against Test Data

Calculated casings parts and rotors temperature distributions during CS and steady-state operation are presented in Fig. 13 for HPIP and LP cylinders. It can be observed that the rise of the turbine metal temperature takes place at all times, starting from the initial moment up to steady-state operation. At the initial phase of the turbine, heating steam goes to the gland seals from the steam header with a temperature of 120 °C. The initial metal temperature is lower than that of the heating steam and during some period of time condensation process takes place in the gland seal regions which are heated by steam saturation temperature, which is lower than the dry steam temperature. That is why at this start-up period the temperature of turbine components grows very slowly.

Validation of the thermal analysis algorithm was done through a comparison with HPIP casing measured data during the turbine

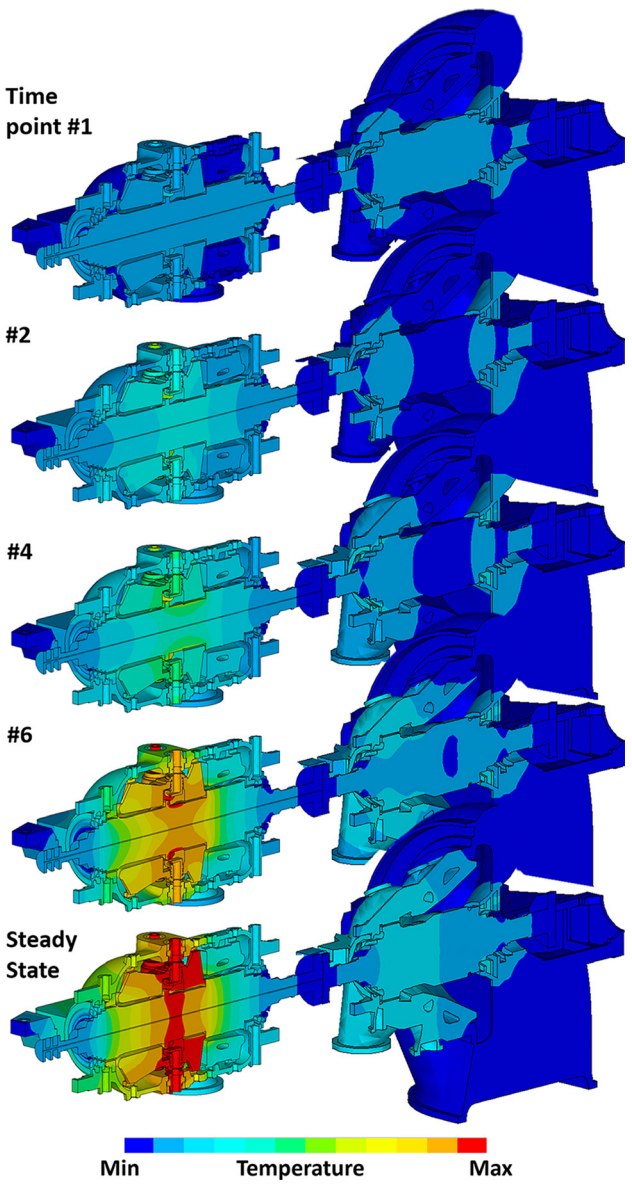

Fig. 13 Turbine components temperatures at CS and steady-state operation

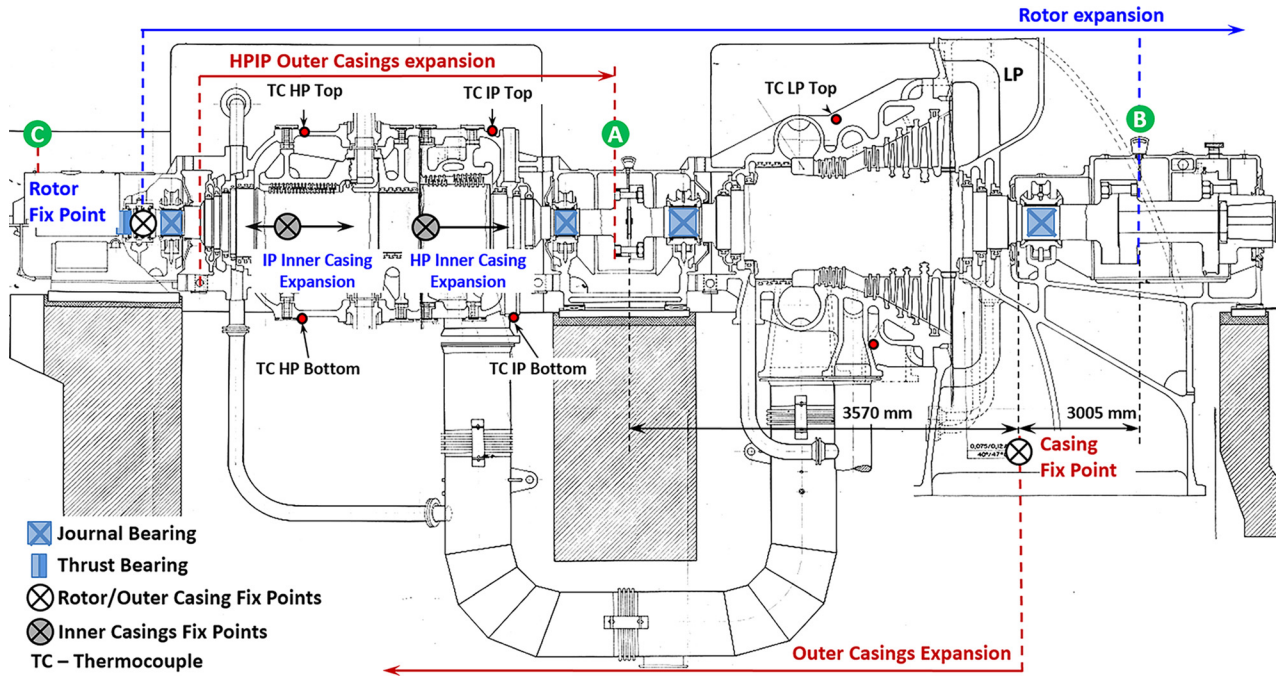

Fig. 14 Turbine unit expansion scheme

commissioning phase. Thermocouples were installed on the casings as it shown in Fig. 14. The comparison of measured temperatures and calculated data for HPIP casing (thermocouple HP top from Fig. 14) is presented in Fig. 15, where the solid line represents measured data and dashed line corresponds to calculated results for HP casing. The comparison shows good agreement between calculated and measured data for all thermocouples installed on HP and IP casing components (calculation results error is less than 5%).

To investigate the effect of condensation on turbine thermal state and expansion, the alternative simulation was performed without interactive algorithm (from Fig. 9) involved. During the whole start-up cycle, no condensation process was assumed, and convection conditions corresponding to noncondensation HTC and dry steam temperatures were applied. The results of this simulation are presented as a dotted line in Fig. 15. Comparison with experimental results shows HPIP casing overheating at the initial phase of start-up, and the difference between measured data and the simulation results reaches up to 20%.

The validation for the casing components thermostructural state is done also against casings thermal expansions. Turbine unit expansion scheme is presented in Fig. 14. Rotor to casing differential expansions were measured at locations "A" for HPIP cylinder and "B" for LP cylinder; HPIP + LP absolute casings expansions were measured at location "C"—see Fig. 14. Comparison of calculated and measured data for the turbine unit at locations C, B, and A is presented in Figs. 16–18.

Calculated absolute and differential expansions according to presented methodology and algorithm (in Fig. 9) are very close to experimentally measured data (less than 1% error). Simulation results without condensation accounting are presented in Fig. 16 by a dotted line. It can be observed that some error take place at the initial phase of start-up.

Another aspect, which was studied, is the effect of blades to rotor thermal contact simulation. The effect of blade roots-to-rotor thermal contact modeling is illustrated in Fig. 18, where comparison of simulation results with measured data is presented. The dashed line of Fig. 18 corresponds to blade roots-to-rotor thermal contact model (see Fig. 12), and dotted line corresponds to a simplified model with no thermal contacts. At the initial phase of heating, results well agree with measured data. But at the time of turbine loading, when steam flow rate increase, the simplified model demonstrates rotor overheating.

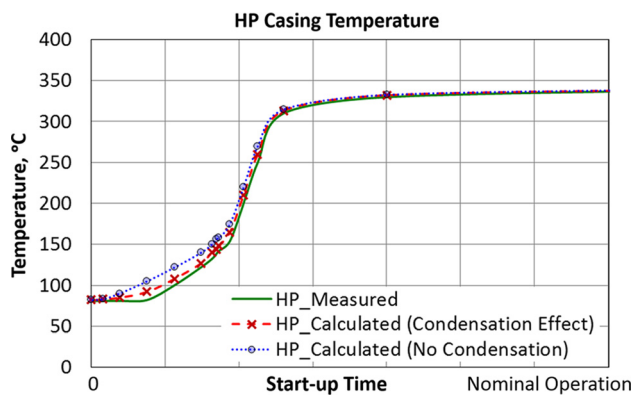

Fig. 15 HP turbine outer casing temperatures

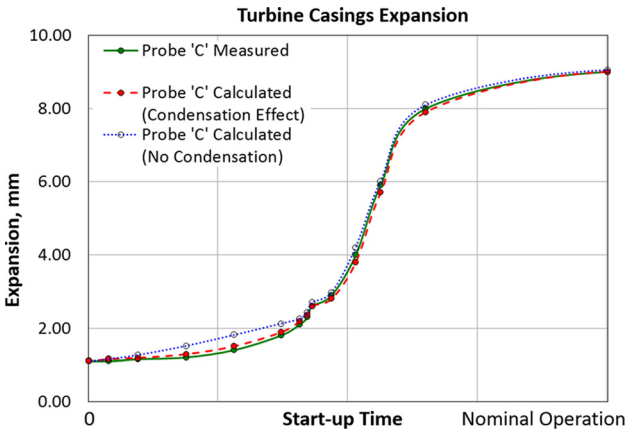

Fig. 16 Turbine unit casings expansion (probe C)

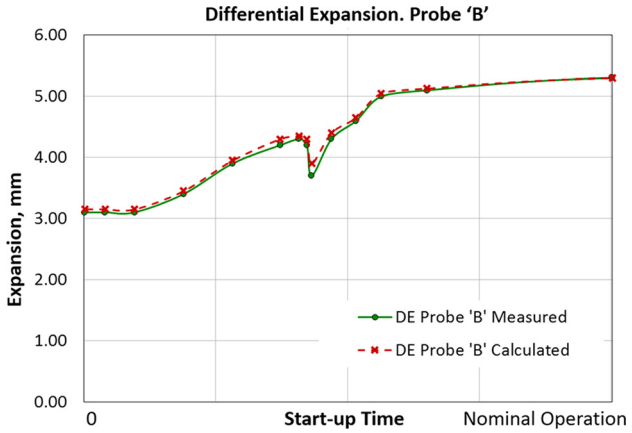

Fig. 17 HPIP and LP rotors to casings differential expansion (probe B)

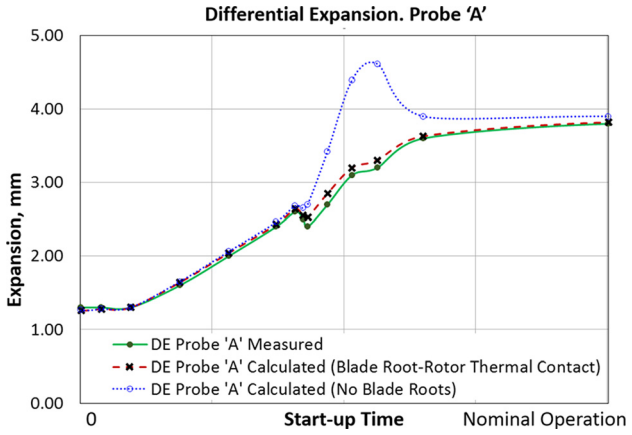

Fig. 18 HPIP rotor to casing differential expansion (probe A)

5 Thermostructural Analysis Results and Discussion

5.1 Thermostresses Analysis Results. The thermal gradients cause thermal stresses which can be observed during transient and steady-state operation and contribute a significant portion of stresses into the entire stress–strain state.

Equivalent stress (plastic study) versus time for the HPIP rotor critical regions #1–#7 (from Fig. 11) are shown in Fig. 19, and the corresponding temperatures are presented in Fig. 20.

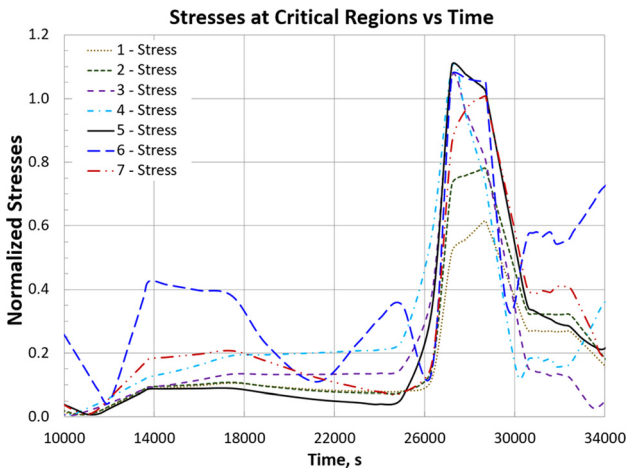

Fig. 19 Equivalent stresses during CS at critical regions

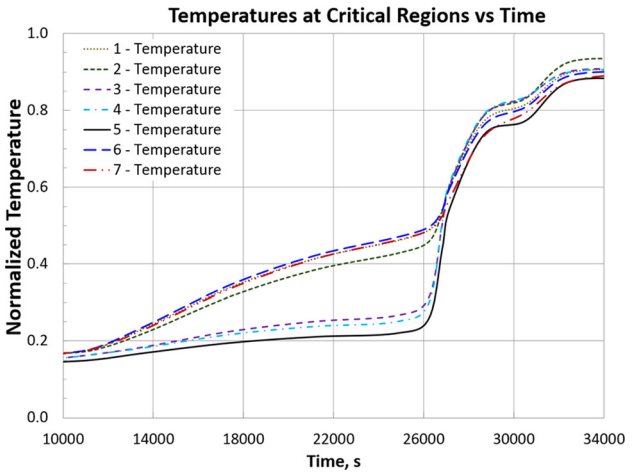

Fig. 20 Temperatures during CS at critical regions

Equivalent stresses (plastic study) distribution during cold start-up and steady-state operation is presented in Fig. 21.

For the considered case, initial casing and rotor metal temperatures close to the steam saturation temperature, which resulted in slow heating at the early phase of start-up. That is why for the current case at the early phase despite condensation process, we did not observe high thermal gradients and stresses, as it was found in other startup cycle simulation, presented in Ref. [11], where turbine components had an ambient initial temperature.

The highest level of thermal gradients and stresses for the current case is observed at the moment of acceleration (time point #5) and ramp-up (time point #6) phases with noncondensation steam conditions (see Figs. 3 and 21).

The peak stresses appear on the disk filets in the region of the steam inlet (points #1 and #2 from Fig. 11), on HP–IP interstage seal (points #3, #4, and #5), and first stage HP blade grooves (corresponding points #6 and #7). Maximum stresses correspond to the points #4 and #6.

5.2 LCF Lifetime Estimation. To estimate unit lifetime, an effective strain range [1], is calculated for the turbine components critical zones. Detailed results for HPIP rotor, as the component which determines unit LCF life, are presented in this paper. The HPIP rotor experimental strain-life curves and detailed material properties which were used for LCF assessment can be found in Ref. [11].

Table 1 shows calculated equivalent total strain range for cold start-up—shut down cycles for each rotor critical point (see Fig. 11) and the corresponding allowable number of cold start-ups. The simulation was performed according to methodology presented in Ref. [11] and taking into the account LCF safety factors.

The analysis shows that maximal total strain range for CS—shut down cycle corresponds to the points #4, #5 (HP–IP interstage seal groves and fillet), and #6 (rotor first stage blade groove). Thus, from a thermomechanical fatigue point of view, for the HPIP rotor and the turbine unit, the number of cold starts is limited to 900 cycles.

6 Conclusions

An integrated approach for thermostructural analysis at transient operations has been validated against a 30 MW turbine unit field experimental data. The influence of different analysis aspects was studied, and the results showed that the following approach refinements are recommended to improve accuracy:

(1) improved accuracy of convection condition simulation by applying direct 1D aerothermodynamic solver, which allows capturing wet versus dry steam properties during

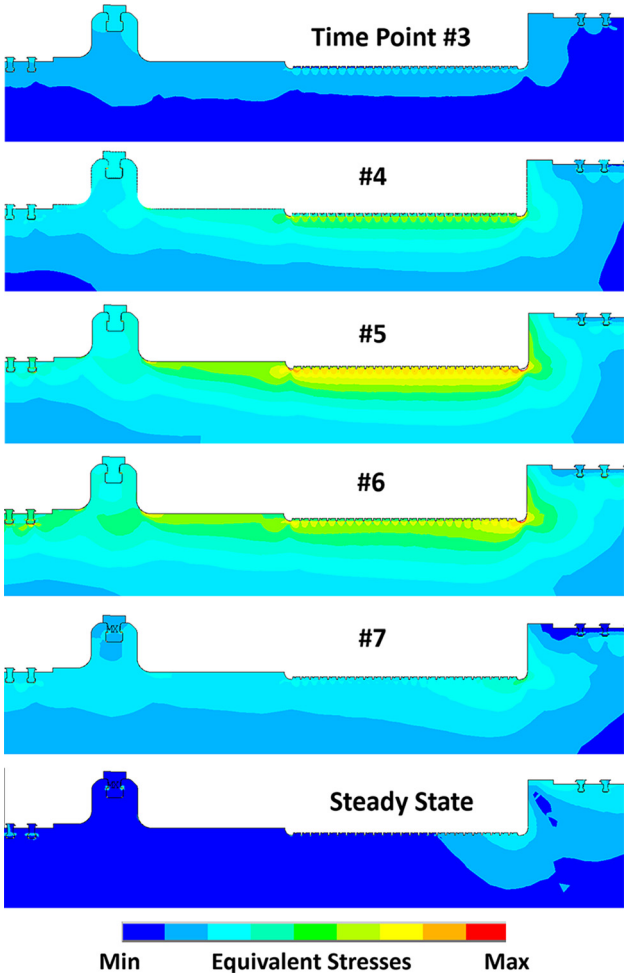

Fig. 21 Equivalent stress distribution in HPIP rotor during CS

Table 1 HPIP rotor LCF lifetime analysis results

Critical zone # (from Fig. 11)	Equivalent total strain range (%)	Allowable number of CS
1	0.12	>50,000
2	0.17	>50,000
3	0.30	15,000
4	0.49	1100
5	0.34	6000
6	0.58	900
7	0.22	>50,000

start-up at each thermal zone and also effect of Windage heating,

(2) differential algorithm for condensation effect prediction and condensation versus noncondensation steam thermal conditions setup,

(3) high level of mechanical model detailing and thermal zones definition,

(4) detailed thermal contacts simulation for all rotor and casing components, and

(5) a high level of automation during all analysis steps helps to accelerate the whole process and improve calculation accuracy.

Acknowledgment

The authors wish to express their gratitude to the many people from the Sulzer Turbo Services Houston, Inc., and SoftInWay, Inc., teams, who contributed their time and efforts to perform this work. The relevance and the strength of the article are based on the invaluable technical support of these people and gratefully acknowledged and appreciated.

Nomenclature

Nu = Nusselt number
Pr = Prandtl number
Re = Reynolds number

References

[1] Manson, S. S., 1966, *Thermal Stress and Low-Cycle Fatigue*, 1st ed., McGraw-Hill, New York.
[2] Incropera, F. P., and Dewitt, D. P., 1996, *Fundamentals of Heat and Mass Transfer*, 5th ed., Wiley, New York.
[3] Kreith, F., 1973, *Principles of Heat Transfer*, 3rd ed., IEP-A Dun-Donnelley, New York.
[4] Nusselt, W., 1916, "Die Oberflächenkondensation des Wasserdampfes," Z. Ver. Dtsch. Ing., **60**(27), pp. 541–546.
[5] Shah, M. M., 1979, "A General Correlation for Heat Transfer During Film Condensation Inside Pipes," Int. J. Heat Mass Transfer, **22**(3), pp. 547–556.
[6] Kubín, M., Hirs, J., and Plasek, J., 2016, "Experimental Analysis of Steam Condensation in Vertical Tube With Small Diameter," Int. J. Heat Mass Transfer, **94**, pp. 403–410.
[7] Uche, J., Artal, J., and Serra, L., 2002, "Comparison of Heat Transfer Coefficient Correlations for Thermal Desalination Units," Desalination, **152**, pp. 195–200.
[8] Matsevity, Y. M., Alyokhina, S. V., Goloschapov, V. N., and Kotulskaja, and O., V., 2012, *Heat Exchange in Construction of Steam Turbines Elements*, NAS of Ukraine, A. N. Podgorny Institute for Mechanical Engineering Problems, Kharkiv, Ukraine.
[9] Maliarenko, V. A., Goloschapov, V. N., Barsukov, V. A., Kotulskaja, O. V., and Chernousenko, O. Y., 1991, *Heat Exchange and Gas Dynamics in Extraction Chambers of Steam Turbines*, Naukova Dumka, Kiev, Ukraine.
[10] Moroz, L., 1989, "Wet Steam Turbines Service Life Diagnostics Based on Its' Thermal State," Ph.D. dissertation, PJSC 'Turboatom,' Kharkiv, Ukraine.
[11] Moroz, L., Frolov, B., and Kochurov, R., 2016, "Steam Turbine Rotor Transient Thermo-Structural Analysis and Lifetime Prediction," ASME Paper No. GT2016-57652.
[12] Born, D., Stein, P., Marinescu, G., Koch, S., and Schumacher, D., 2016, "Thermal Modeling of an Intermediate Pressure Steam Turbine by Means of Conjugate Heat Transfer—Simulation and Validation," ASME Paper No. GT2016-57247.
[13] Pusch, D., Voigt, M., Vogeler, K., Dumstorff, P., and Almstedt, H., 2016, "Setup, Validation and Probabilistic Robustness Estimation of a Model for Prediction of LCF in Steam Turbine Rotors," ASME Paper No. GT2016-57321.
[14] Moroz, L., Govorushchenko, Y., Pagur, P., Grebennik, K., Kutrieb, W., and Kutrieb, M., 2011, "Integrated Environment for Gas Turbine Preliminary Design," Osaka International Gas Turbine Congress, Osaka, Japan, Nov. 13–18, Paper No. IGTC2011-0007.
[15] Brilliant, H. M., and Tolpadi, A. K., 2004, "Analytical Approach to Steam Turbine Heat Transfer in a Combined Cycle Power Plant," ASME Paper No. GT2004-53387.
[16] Mallick, A. R., 2014, *Practical Boiler Operation Engineering and Power Plant*, 3rd ed., PHI Learning Private Limited, Delhi, India.